Relative Strength of Cation−π vs Salt−Bridge Interactions: The G t α(340−350) Peptide/Rhodopsin System

ARTICLE *in* JOURNAL OF THE AMERICAN CHEMICAL SOCIETY · JULY 2006

Impact Factor: 12.11 · DOI: 10.1021/ja058513z · Source: PubMed

7 AUTHORS, INCLUDING:

Matthew A Anderson
Algenol Biofuels
13 PUBLICATIONS **214** CITATIONS
SEE PROFILE

Rieko Arimoto
Vertex Pharmaceuticals
14 PUBLICATIONS **384** CITATIONS
SEE PROFILE

David Cistola
University of North Texas HSC at Fort Worth
68 PUBLICATIONS **2,951** CITATIONS
SEE PROFILE

Garland R Marshall
Washington University in St. Louis
376 PUBLICATIONS **10,154** CITATIONS
SEE PROFILE

J|A|C|S
ARTICLES
Published on Web 05/19/2006

Relative Strength of Cation-π vs Salt-Bridge Interactions: The $G_t\alpha(340-350)$ Peptide/Rhodopsin System

Matthew A. Anderson,[†] Benhur Ogbay,[†] Rieko Arimoto,[†,§] Wei Sha,[†,||] Oleg G. Kisselev,[‡] David P. Cistola,[†] and Garland R. Marshall*[,†]

Contribution from the Department of Biochemistry and Molecular Biophysics, Washington University School of Medicine, St. Louis, Missouri 63110, and Department of Ophthalmology and Department of Biochemistry and Molecular Biology, Saint Louis University School of Medicine, St. Louis, Missouri 63104

Received December 23, 2005; E-mail: garland@pcg.wustl.edu

Abstract: Interactions between cationic and aromatic side chains of amino acid residues, the so-called cation$-\pi$ interaction, are thought to contribute to the overall stability of the folded structure of peptides and proteins. The transferred NOE NMR structure of the $G_t\alpha(340-350)$ peptide bound to photoactivated rhodopsin (R*) geometrically suggests a cation$-\pi$ interaction stabilizing the structure between the ϵ-amine of Lys341 and the aromatic ring of the C-terminal residue, Phe350. This interaction has been explored by varying substituents on the phenyl ring to alter the electron density of the aromatic ring of Phe350 and observing the impact on binding of the peptide to R*. The results suggest that while a cation$-\pi$ interaction geometrically exists in the $G_t\alpha(340-350)$ peptide when bound to R*, its energetic contribution to the stability of the receptor-bound structure is relatively insignificant, as it was not observed experimentally. The presence of an adjacent and competing salt-bridge interaction between the ϵ-amine of Lys341 and the C-terminal carboxylate of Phe350 effectively shields the charge of the ammonium group. Experimental data supporting a significant cation$-\pi$ interaction can be regained through a series of Phe350 analogues where the C-terminal carboxyl has been converted to the neutral carboxamide, thus eliminating the shielding salt-bridge. TrNOE NMR experiments confirmed the existence of the cation$-\pi$ interaction in the carboxamide analogues. Various literature estimates of the strength of cation$-\pi$ interactions, including some that estimate strengths in excess of salt-bridges, are compromised by omission of the relevant anion in the calculations.

Introduction

Hydrogen bonds, hydrophobic interactions, and salt-bridges are all known to provide stability and specificity to the folded structure of proteins. In addition to these traditional noncovalent interactions, the cation$-\pi$ interaction[1,2] has increasingly been suggested as important and relevant in protein structure, binding, and catalytic function. Extensive studies of the cation$-\pi$ interaction have been performed involving host$-$guest systems, theoretical studies, and gas-phase experiments, establishing the interaction as a potentially significant force in molecular recognition [For a recent review, see Meyer et al.[3]]. The importance of cation$-\pi$ interactions to biological systems has been demonstrated by mutation studies in proteins and analysis of crystal structure data.[4−7] Only recently have cation$-\pi$ interactions been studied in peptide model systems.[8−19] These studies show that a cation$-\pi$ interaction between a side-chain protonated amine (Lys or Arg) and an aromatic ring (Phe, Trp, or Tyr) can stabilize the folded structure of a peptide just as in proteins.

Rhodopsin/transducin is the prototypical and most widely studied G protein-coupled receptor (GPCR)/G protein system. Although the crystal structures of various G proteins[20−26] and

[†] Washington University School of Medicine.
[‡] Saint Louis University School of Medicine.
[§] Current address: Vertex Pharmaceuticals, Inc., Cambridge, MA 02139.
[||] Current address: Science Applications International Corporation (SAIC), Rockville, MD 20850.

(1) Ma, J. C.; Dougherty, D. A. *Chem. Rev.* **1997**, *97*, 1303−1324.
(2) Scrutton, N. S.; Raine, A. R. *Biochem. J.* **1996**, *319* (Pt 1), 1−8.
(3) Meyer, E. A.; Castellano, R. K.; Diederich, F. *Angew. Chem., Int. Ed.* **2003**, *42*, 1210−1250.
(4) Burley, S. K.; Petsko, G. A. *FEBS Lett.* **1986**, *203*, 139−143.
(5) Singh, J.; Thornton, J. M. *J. Mol. Biol.* **1990**, *211*, 595−615.
(6) Gallivan, J. P.; Dougherty, D. A. *Proc. Natl. Acad. Sci. U.S.A.* **1999**, *96*, 9459−9464.
(7) Flocco, M. M.; Mowbray, S. L. *J. Mol. Biol.* **1994**, *235*, 709−717.
(8) Fernandez-Recio, J.; Vazquez, A.; Civera, C.; Sevilla, P.; Sancho, J. *J. Mol. Biol.* **1997**, *267*, 184−197.
(9) Burghardt, T. P.; Juranic, N.; Macura, S.; Ajtai, K. *Biopolymers* **2002**, *63*, 261−272.
(10) Orner, B. P.; Salvatella, X.; Sanchez Quesada, J.; De Mendoza, J.; Giralt, E.; Hamilton, A. D. *Angew. Chem., Int. Ed.* **2002**, *41*, 117−119.
(11) Olson, C. A.; Shi, Z.; Kallenbach, N. R. *J. Am. Chem. Soc.* **2001**, *123*, 6451−6452.
(12) Shi, Z.; Olson, C. A.; Kallenbach, N. R. *J. Am. Chem. Soc.* **2002**, *124*, 3284−3291.
(13) Pletneva, E. V.; Laederach, A. T.; Fulton, D. B.; Kostic, N. M. *J. Am. Chem. Soc.* **2001**, *123*, 6232−6245.
(14) Tsou, L. K.; Tatko, C. D.; Waters, M. L. *J. Am. Chem. Soc.* **2002**, *124*, 14917−14921.
(15) Slutsky, M. M.; Marsh, E. N. *Protein Sci.* **2004**, *13*, 2244−2251.
(16) Tatko, C. D.; Waters, M. L. *Protein Sci.* **2003**, *12*, 2443−2452.
(17) Andrew, C. D.; Penel, S.; Jones, G. R.; Doig, A. J. *Proteins* **2001**, *45*, 449−455.
(18) Andrew, C. D.; Bhattacharjee, S.; Kokkoni, N.; Hirst, J. D.; Jones, G. R.; Doig, A. J. *J. Am. Chem. Soc.* **2002**, *124*, 12706−12714.
(19) Tatko, C. D.; Waters, M. L. *J. Am. Chem. Soc.* **2004**, *126*, 2028−2034.

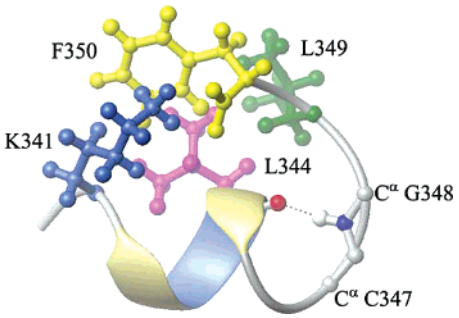

Figure 1. Ribbon diagram of R*-bound $G_t\alpha(340-350)$ based on the TrNOE structure (PDB 1AQG[32]). Prepared with MOLMOL.[59]

dark-adapted rhodopsin (R), the GPCR in vision, have been solved,[27,28] an atomic view of the interaction between photoactivated rhodopsin (R*) and its G protein transducin (G_t) remains undefined. The visual signal transduction cascade is initiated when the GDP-bound form of the heterotrimeric G protein transducin ($G_t\alpha\beta\gamma$) binds to the light-activated Meta II (MII) state of R*. The C-terminal eleven residues of transducin's α-subunit, 340−350, has been identified as a significant recognition motif in binding to R*, and a synthetic undecapeptide corresponding to $G_t\alpha(340-350)$ (IKENLKDCGLF) can mimic the effects of transducin, by binding to photoactivated rhodopsin and stabilizing the MII state.[29,30]

The R*-bound structure of the C-terminal α-peptide (340−350) of G_t was determined previously by transferred nuclear Overhauser effect (TrNOE) NMR spectroscopy.[31,32] Our studies[32] demonstrated that $G_t\alpha(340-350)$ binds to photoactivated rhodopsin, forming a reverse glycine C-cap turn,[33] with a prominent hydrophobic cluster of four residues, specifically K341, L344, L349, and F350 (Figure 1). These residues are conserved in the majority of G protein subclasses, suggesting that this motif may be significant in G protein/GPCR interactions, at least for the rhodopsin family of GPCRs (Table 1, all Gα-subunit sequences with the exception of G_z, G_s, and G_{olf} have an aromatic residue (phenylalanine (F) or tyrosine (Y)) at the C-terminal position and a lysine (K) at position 341 with the additional exception of G_o). Furthermore, the corresponding C-terminal region in the crystal structure of $G_i\alpha$ bound to RGS4[22] showed a conformation for the C-terminal segment identical to the TrNOE-derived structure[32] suggesting that the observed TrNOE structure of the R*-bound undecapeptide was energetically favored in the intact protein in that particular complex. In addition, a structure determined recently by TrNOE studies[34] using an analogue of the $G_t\alpha(340-350)$ sequence with two mutations, K341R and C347S, is in excellent agreement with our results[32] except for the cation−π interaction that is sterically incompatible with the K341R mutation. In a recent study, Abdulaev and co-workers[35] have grafted segments from the cytoplasmic face of bovine opsin onto a surface loop of a mutant form of thioredoxin and shown partial transducin activation. More recently, Barbazon et al.[36] have studied the interaction of the $G_t\alpha(340-350)$ with this R*-mimetic by TrNOE NMR and showed that only the Gly C-cap backbone conformation was similar in the thioredoxin model system with no evidence of a helical structuring of the N-terminal segment as seen with native R* in the Kisselev[32] or Koenig[34] studies discussed above.

Table 1. Sequence Comparison of C-Terminal Peptide Segments of α-Subunits of Different G Proteins

Protein	G_αAA #	AA Sequence[a]									
G_{tr}	340-350	I	K	E	N	L	K	D	C	G	L	F
G_{tc}	343-353	I	K	E	N	L	K	D	C	G	L	F
G_{gust}	344-354	I	K	E	N	L	K	D	C	G	L	F
G_o	344-354	I	A	N	N	L	R	G	C	G	L	Y
G_{i1}	344-354	I	K	N	N	L	K	D	C	G	L	F
G_{i2}	345-355	I	K	N	N	L	K	D	C	G	L	F
G_{i3}	344-354	I	K	N	N	L	K	E	C	G	L	Y
G_z	345-355	I	Q	N	N	L	K	Y	I	G	L	C
G_s	384-394	Q	R	M	H	L	R	Q	Y	E	L	L
G_{olf}	371-381	Q	R	M	H	L	R	Q	Y	E	L	L

[a] Note the high conservation of amino acid residues (I, N, L, C, G) (blue) suggesting a function role for the C-terminal segment of the α-subunit. Residues that are identical to $G_t\alpha$ are highlighted.

In the TrNOE structure of $G_t\alpha(340-350)$,[32] we observed that the proximity of the ϵ-amine of Lys341 to the aromatic ring of Phe350 suggests a possible cation−π interaction stabilizing the structure (Figure 2) as well as a salt-bridge between the C-terminal carboxylate of Phe350 and the ϵ-amino group of Lys341. Theoretical studies by Gallivan and Dougherty[37] suggested that a cation−π interaction in solvent with a protein-like dielectric (ethyl acetate, $\epsilon = 5.99$) contribute maximally −6.2 kcal/mol to the free energy (ΔG) of the system. By their calculations, the cation−π interaction was relatively insensitive to dielectric since the calculated value in water ($\epsilon = 78$) was only reduced to −5.5 kcal/mol. The value for the salt bridge was −19.7 kcal/mol in ethyl acetate and reduced to −2.2 kcal/mol in water in agreement with Coulomb's law. Additional gas-phase calculations by Mo et al.[38] estimated the intermolecular

(20) Coleman, D. E.; Sprang, S. R. *Biochemistry* **1998**, *37*, 14376−14385.
(21) Lambright, D. G.; Sondek, J.; Bohm, A.; Skiba, N. P.; Hamm, H. E.; Sigler, P. B. *Nature* **1996**, *379*, 311−319.
(22) Tesmer, J. J.; Berman, D. M.; Gilman, A. G.; Sprang, S. R. *Cell* **1997**, *89*, 251−261.
(23) Wall, M. A.; Coleman, D. E.; Lee, E.; Iniguez-Lluhi, J. A.; Posner, B. A.; Gilman, A. G.; Sprang, S. R. *Cell* **1995**, *83*, 1047−1058.
(24) Noel, J. P.; Hamm, H. E.; Sigler, P. B. *Nature* **1993**, *366*, 654−663.
(25) Lambright, D. G.; Noel, J. P.; Hamm, H. E.; Sigler, P. B. *Nature* **1994**, *369*, 621−628.
(26) Sondek, J.; Lambright, D. G.; Noel, J. P.; Hamm, H. E.; Sigler, P. B. *Nature* **1994**, *372*, 276−279.
(27) Palczewski, K. et al. *Science* **2000**, *289*, 739−745.
(28) Teller, D. C.; Okada, T.; Behnke, C. A.; Palczewski, K.; Stenkamp, R. E. *Biochemistry* **2001**, *40*, 7761−7772.
(29) Hamm, H. E.; Deretic, D.; Arendt, A.; Hargrave, P. A.; Koenig, B.; Hofmann, K. P. *Science* **1988**, *241*, 832−835.
(30) Aris, L.; Gilchrist, A.; Rens-Domiano, S.; Meyer, C.; Schatz, P. J.; Dratz, E. A.; Hamm, H. E. *J. Biol. Chem.* **2001**, *276*, 2333−2339.
(31) Dratz, E. A.; Furstenau, J. E.; Lambert, C. G.; Thireault, D. L.; Rarick, H.; Schepers, T.; Pakhlevaniants, S.; Hamm, H. E. *Nature* **1993**, *363*, 276−281.
(32) Kisselev, O. G.; Kao, J.; Ponder, J. W.; Fann, Y. C.; Gautam, N.; Marshall, G. R. *Proc. Natl. Acad. Sci. U.S.A.* **1998**, *95*, 4270−4275.
(33) Schellman, C. In *Protein Folding*; Jaenicke, R., Ed.; Elsevier/North-Holland Biomedical Press: Amsterdam, 1980; pp 53−61.
(34) Koenig, B. W.; Kontaxis, G.; Mitchell, D. C.; Louis, J. M.; Litman, B. J.; Bax, A. *J. Mol. Biol.* **2002**, *322*, 441−461.
(35) Abdulaev, N. G.; Ngo, T.; Chen, R.; Lu, Z.; Ridge, K. D. *J. Biol. Chem.* **2000**, *275*, 39354−39363.
(36) Brabazon, D. M.; Abdulaev, N. G.; Marino, J. P.; Ridge, K. D. *Biochemistry* **2003**, *42*, 302−311.
(37) Gallivan, J. P.; Dougherty, D. A. *J. Am. Chem. Soc.* **2000**, *122*, 870−874.

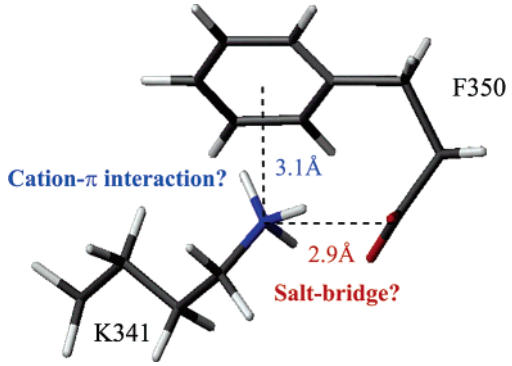

Figure 2. Proximity of Lys341 side chain ϵ-amine to Phe350 showing cation−π and salt-bridge interactions. Prepared with MOLMOL[59] from PDB 1AQG.[32] The average distance for the ensemble of structures with SD is 3.1 ± 0.05 Å for the cation−π interaction and 2.89 ± 0.2 Å for the salt-bridge.

interaction energy at between −6 and −12 kcal/mol for a series of nonbonded complexes of N-substituted piperidines and substituted monocyclic aromatics and suggested that the interaction had significant polarization and charge-transfer components. We hypothesized that if the contribution of a cation−π interaction is so energetically favorable, perturbation of the interaction should be observable by measurement of binding affinity in a biological assay. On the other hand, Hunter et al.[39,40] estimated the energy of a pyridinium cation−π interaction in chloroform (ϵ = ∼4−5) at only −2.5 ± 0.4 kJ/mol or −0.6 ± 0.1 kcal/mol by a chemical double-mutant cycle, in agreement with experimental studies on the modeled system. Bartoli and Roelens[41] showed both experimentally and computationally that the counteranion has a dramatic effect on the strength of the interaction in a cation−π interaction in a model lipophilic cyclophane system with a series of tetramethylammonium (TMA) and acetylcholine salts in $CDCl_3$. The charge dispersion on the anion was a major factor in determining the influence of the anion on the strength of the cation−π interaction. An anion with a diffuse negative charge such as picrate yielded a ΔG of approximately −2 kcal/mol for the cation−π interaction in chloroform, but an anion with a more concentrated charge such as acetate, which corresponds to the C-terminal carboxylate of Gtα(340−350), limited the ΔG of the interaction to approximately −0.6 kcal/mol in $CDCl_3$.

Other experimental estimates of the interaction strength of cation−π interactions have come from model peptide studies. Fernandez-Recio et al.[8] studied the interaction between tryptophan and histidine pairs in either the *i* and *i* + 3 or *i* and *i* + 4 positions in an α-helix. Helix stabilization was only seen with Trp/His^+ in the *i*/*i* + 4 orientation and estimated at −1 kcal/mol. Tsou et al.[14] estimated the extent of α-helix stabilization by the interaction between a protonated amine (lysine, ornithine, and diaminobutyric acid) and the phenyl ring of phenylalanine in water as −0.4 kcal/mol, seen only in the Phe-Orn case. Similar studies using a designed β-hairpin to orient the interacting residues measured interaction energies between Phe or Trp and Lys or Arg in diagonal positions on the β-hairpin at between −0.20 and −0.48 kcal/mol.[16]

It has been suggested by several groups[15,17,18] that observed cation−π interactions are more hydrophobic in nature than electrostatic. Slutsky and Marsh[15] used a model coil−coil peptide to estimate the interaction between Arg and Phe/Trp/Tyr. Only the Arg/Phe combination proved more stable than the control, Lys/Glu, and the authors suggested that hydrophobic packing of Arg side-chain methylenes rather than a cation−π interaction was responsible. Other studies by Andrew et al.[17] of interactions between Val/Ile and Lys/Arg in the *i* and *i* + 4 positions found helix stabilizations between −0.14 and −0.32 kcal/mol. In addition, the nonpolar/polar pairs Ile-Lys, Ile-Arg, and Val-Lys occur in protein helices more often than expected. Phe-Lys, Lys-Phe, Phe-Arg, Arg-Phe, and Tyr-Lys are all stabilizing by −0.10 to −0.18 kcal/mol when placed *i*, *i* + 4 on the surface of a helix in aqueous solution.[18] The similarity in the experimental values for helix stabilization between nonaromatic hydrophobic side chains such as Val and Ile and aromatic side chains with Arg and Lys suggest that much of the stabilization energy measured for aromatic residues with Lys/Arg may simply arise from hydrophobic forces rather than cation−π stabilization alone. However, in a recent study,[19] Tatko and Waters compared the interaction of norleucine (Nle) and Lys with Phe, Trp, or Cha (α-cyclohexylalanine) in the diagonal positions of a designed β-hairpin and found that interaction energies between Lys and Phe or Trp were between −0.2 and −0.4 kcal/mol. The interaction energies between Nle and Phe or Trp were slightly less favorable (−0.1 to −0.2 kcal/mol). The NMR and thermal denaturation studies showed that the Lys side chain interacts in a specific manner with Phe or Trp through the polarized C_ϵ, and Nle does not interact in a specific manner with either aromatic side chain. These results indicate that Lys and Nle interact in fundamentally different ways with aromatic residues, arguing that observed cation−π interactions are not predominately hydrophobic in nature.

The debate about the strength of cation−π interactions and their role in protein/peptide folding is ongoing and multifaceted; while there is little doubt about the importance of the cation−π interaction among noncovalent forces, considerable controversy exists regarding the relative strengths of interaction. The large differences in energetics predicted by calculations and the question of the relative strengths of cation−π versus salt-bridge interactions prompted an experimental study of the Gtα(340−350)/R* system in which both were present (Figure 2). In this study, two series of peptides were synthesized to perturb the putative cation−π interaction between the ϵ-amine of Lys341 and the aromatic ring of Phe350 and to determine what the relative role of the two interactions is in stabilizing the R*-bound conformation of Gtα(340−350).

Materials And Methods

Design of Peptide Analogues. Two series of peptides were synthesized for this study; the sequences are shown in Table 2. Series I investigated the role of the cation−π interaction suggested in the TrNOE structure of the Gtα(340−350) peptide. The peptide analogues in Series I contain a variety of substitutions at the *para* position of Phe350: peptides 1 and 4 contain electron-donating groups, Tyr and Phe(*p*-NH_2); peptides 3 and 5 contain electron-withdrawing groups, Phe(*p*-F) and Phe(*p*-NO_2); peptide 2 contains Trp (indole ring system) at position 350, and peptide 6 has Cha (α-cyclohexylalanine) at position 350 which lacks a π-system as a further control.

(38) Mo, Y.; Subramanian, G.; Gao, J.; Ferguson, D. M. *J. Am. Chem. Soc.* **2002**, *124*, 4832−4837.
(39) Hunter, C. A.; Low, C. M.; Rotger, C.; Vinter, J. G.; Zonta, C. *Proc. Natl. Acad. Sci. U.S.A.* **2002**, *99*, 4873−4876.
(40) Hunter, C. A.; Low, C. M.; Rotger, C.; Vinter, J. G.; Zonta, C. *Chem. Commun. (Camb)* **2003**, 834−835.
(41) Bartoli, S.; Roelens, S. *J. Am. Chem. Soc.* **2002**, *124*, 8307−8315.

Table 2. Sequences and Calculated EC_{50} Values with SE of the Peptide Analogues[a]

peptide	sequence	$EC_{50} \pm SE$[b] (μM)
$G_t\alpha$ native	IKENLKDCGLF−OH	530 ± 90
	Series I (Carboxylates)	
1	IKENLKDCGL**Y**−OH	840 ± 40
2	IKENLKDCGL**W**−OH	540 ± 50
3	IKENLKDCGL**F(*p*-F)**−OH	440 ± 20
4	IKENLKDCGL**F(*p*-NH_2)**−OH	1670 ± 70
5	IKENLKDCGL**F(*p*-NO_2)**−OH	420 ± 20
6	IKENLKDCGL**(Cha)**−OH	200 ± 10
	Series II (Carboxamides)	
7	IKENLKDCGL**F(*p*-NO_2)**−NH_2	980 ± 80
8	IKENLKDCGL**F(−F_5)**−NH_2	1830 ± 530
9	IKENLKDCGL**Y**−NH_2	730 ± 240
10	IKENLKDCGL**Y(Me)**−NH_2	490 ± 100
11	IKENLKDCGL**(2-Nal)**−NH_2	220 ± 70
12	IKENLKDCGL**F(*p*-*tert*-butyl)**−NH_2	110 ± 20
13	IKENLKDCGL**(Cha)**−NH_2	190 ± 40
14	IKENLKDCGLF−NH_2	320 ± 70
15	IKENLKDCGL**F(2-Cl)**−NH_2	490 ± 90
16	IKENLKDCGL**F(2-NO_2)**−NH_2	2020 ± 230

[a] Modifications from the native peptide are indicated in bold. [b] EC_{50} values for each peptide ± standard error (SE) were calculated using GraphPad Prism.

The peptides in Series II were designed subsequent to biological assay of Series I, to address the possibility that an adjacent salt-bridge interaction between the carboxylate of Phe350 and the ϵ-amine of Lys341 shielded and prevented observation of the cation−π interaction. These analogues were similar to those in Series I, with the following modifications. First, the charged C-terminal carboxylate was changed to a carboxamide in all compounds to neutralize the negative charge and eliminate the salt-bridge interaction with the ϵ-amino group of Lys341. Second, the number of peptides in the series was increased to provide better sampling of the variability in the electronic perturbation of the aromatic ring at Phe 350. Namely, we substituted pentafluoro-Phe (Phe(−F_5)) for the *p*-F−Phe used in Series I, omitted Trp, added 2-naphthylalanine (2-Nal) as an extended π-system, and added two *ortho*-substituted Phe analogues Phe(2-Cl) and Phe(2-NO_2) as well as two analogues with increased hydrophobicity and modest electron-donating ability (Tyr(Me) and Phe(-*p*-*tert*-butyl)).

Peptide Synthesis. All reagents were obtained from commercial suppliers and used without further purification. Analogue peptides were synthesized with standard solid-phase methodology by manual Fmoc or Boc strategy. Peptides **1** and **2** of Series I were synthesized by Boc strategy on Pam Resin preloaded with Boc-Tyr(2-Br-Z) (0.70 mmol/g) and Boc-Trp(CHO) (0.84 mmol/g), respectively. Boc strategy couplings were achieved with 4 equiv of Boc-amino acids, 3.8 equiv of 2-(1*H*-benzotriazole-1-yl)-1,1,3,3-tetramethyluronium hexafluorophosphate (HBTU), and 6 equiv of diisopropylethylamine (DIPEA). The Boc groups were deprotected by treatment with 50% trifluoroacetic acid (TFA) in dichloromethane (DCM). The crude peptides **1** and **2** were cleaved from the resin by hydrofluoric acid (HF) and scavengers (5% anisol, 2.5% 1,2-ethanedithiol (EDT)). Formyl protection of Trp in peptide **2** was removed by treating with piperidine (10% in DMF) at 0 °C before HF cleavage. The remaining peptides in Series I were synthesized by Fmoc strategy on Wang resin (0.58 mmol/g). For each peptide, the C-terminal amino acid (2 equiv) was first coupled to Wang resin catalyzed by 2,6-dichlorobenzyl chloride (2 equiv) and pyridine (3 equiv) in DMF,[42] followed by capping excess reactive groups on the resin with benzoyl chloride. Subsequent Fmoc-amino acids (4 equiv) in peptides **3**−**6** were coupled to resin with HBTU (4 equiv), *N*-hydroxybenzotriazole (HOBT) (4 equiv), and DIPEA (8 equiv).

The peptides in Series II were synthesized by Fmoc strategy on Rink Amide-MBHA resin (0.73 mmol/g) obtained from NovaBiochem (San Diego, CA). Fmoc deprotections were performed by treatment with 20% piperidine in *N*,*N*′-dimethylformamide (DMF) for 20 min at room temperature. All Fmoc strategy couplings were accomplished with 3 equiv each of Fmoc amino acid, HBTU, and DIPEA in DMF (2 mL). Coupling reactions were run for 1−3 h. The resin was washed with DMF and DCM. Coupling efficiencies were monitored by a Kaiser test.[43] After a positive Kaiser test, the coupling was repeated.

All Fmoc strategy peptides were cleaved from the resin by treatment with a mixture of 88.5% TFA, 5% H_2O, 2.5% EDT, and 4% triisopropylsilane (TIS) for 1−2 h at room temperature. After filtration, TFA was removed by evaporation and the crude peptides precipitated with diethyl ether.

Peptides were purified by reversed-phase HLPC. Samples were prepared by dissolving the peptides in a 1:1 mixture of Solvent A (0.05% TFA in H_2O) and Solvent B (0.038% TFA, 10% H_2O in acetonitrile). The samples were then monitored at 220 nm with a Rainin HPXL solvent delivery system and a Rainin Dynamax UV-1 absorbance detector (Varian, Palo Alto, CA). A preparative Rainin Dynamax C_{18}-column (Varian, Palo Alto, CA) was used with a linear gradient of Solvent A to Solvent B, 10−100% B over 25 min, flow rate 15 mL/min. Peptide identity was confirmed by electrospray mass spectrometry at the Protein and Nucleic Acid Chemistry Laboratory, Washington University School of Medicine, St. Louis. Table 3 lists the calculated and found mass peaks for the Series II peptides.

Table 3. ESI-MS Results for the Series II Peptides

peptide	molecular formula	calculated mass [M + H^+]	found mass
7	$C_{57}H_{94}N_{16}O_{18}S$	1323.66	1323.7
8	$C_{57}H_{90}F_5N_{15}O_{16}S$	1368.63	1368.4
9	$C_{57}H_{95}N_{15}O_{17}S$	1294.67	1294.6
10	$C_{58}H_{97}N_{15}O_{17}S$	1308.69	1308.6
11	$C_{61}H_{97}N_{15}O_{16}S$	1328.70	1328.7
12	$C_{61}H_{103}N_{15}O_{16}S$	1337.74	1334.7
13	$C_{57}H_{101}N_{15}O_{16}S$	1284.73	1284.7
14	$C_{57}H_{95}N_{15}O_{16}S$	1278.68	1278.6
15	$C_{57}H_{94}ClN_{15}O_{16}S$	1312.64	1312.7
16	$C_{57}H_{94}N_{16}O_{18}S$	1323.67	1323.7

"Extra" Meta II Assay. The absorbance spectra of rhodopsin in rod outer segments were measured in the presence of varying concentrations of $G_t\alpha(340-350)$ analogues using a Cary50 spectrophotometer (Varian, Palo Alto, CA), essentially as described previously.[44−46] The assay samples contained 200 μg/mL (~5 μM) of rhodopsin in rod outer-segment membranes, prepared as described,[47,48] and analogue peptides in Buffer A (pH 8.0, 20 mM Tris/HCl, 130 mM NaCl, 1 mM $MgCl_2$, 1 μM EDTA, 2 mM dithiothreitol (DTT)). The samples were kept on ice at 0 °C and prepared under dim red light to avoid premature bleaching of rhodopsin. The absorption spectrum of dark-adapted rhodopsin was taken, and rhodopsin was activated by 490 ± 5 nm light for 20 s, followed by a scan acquiring the second spectrum. The cuvette compartment was maintained at 4 °C, and the path length was 10 mm. The measurements were repeated in triplicate with increasing concentration of analogue peptides from 1 μM to 5 mM. As a control, rhodopsin was bleached overnight at 4 °C and added to an aliquot of peptide at each concentration followed by absorbance spectrum collection as described above. The amount of "extra" Meta II was

(42) Sieber, P. *Tetrahedron Lett.* **1987**, *28*, 6147−6150.
(43) Kaiser, E.; Colescott, R. L.; Bossinger, C. D.; Cook, P. I. *Anal. Biochem.* **1970**, *34*, 595−598.
(44) Kisselev, O. G.; Ermolaeva, M. V.; Gautam, N. *J. Biol. Chem.* **1994**, *269*, 21399−21402.
(45) Kisselev, O. G.; Meyer, C. K.; Heck, M.; Ernst, O. P.; Hofmann, K. P. *Proc. Natl. Acad. Sci. U.S.A.* **1999**, *96*, 4898−4903.
(46) Arimoto, R.; Kisselev, O. G.; Makara, G. M.; Marshall, G. R. *Biophys. J.* **2001**, *81*, 3285−3293.
(47) Papermaster, D. S.; Dreyer, W. J. *Biochemistry* **1974**, *13*, 2438−2444.
(48) Yamazaki, A.; Bartucca, F.; Ting, A.; Bitensky, M. W. *Proc. Natl. Acad. Sci. U.S.A.* **1982**, *79*, 3702−3706.

calculated as $\Delta A_{380nm} - \Delta A_{417nm}$, where ΔA is the absorbance change before and after light activation (380 nm = λ_{max} of MII, 417 nm = isobestic point of MI/MII).

Dose−response curves for the G$_t$α(340−350) peptide analogues were analyzed by nonlinear regression with GraphPad Prism (Version 3.03 for Windows, GraphPad Software, San Diego California USA, www.graphpad.com) using the following equation to obtain EC_{50} values ± SE.

$$\text{Meta II} = \text{Baseline} + \text{Range} \times \left(\frac{[\text{Peptide}]}{[\text{Peptide}] + EC_{50}}\right) \quad (1)$$

Baseline is the asymptotic minimum absorbance, *Range* is the asymptotic maximum absorbance minus the *Baseline*, *[Peptide]* is the concentration of peptide, and *EC$_{50}$* is the concentration that gives a response halfway between *Baseline* and (*Baseline* + *Range*).

Calculation of Hammett Substituent Constants. To estimate the electron density of the benzene ring on the side chain at position 350 we used the Hammett equation,[49]

$$\log\frac{K_a}{K_a^\circ} = \rho\sigma \quad (2)$$

where $K_a°$ is the ionization constant of benzoic acid in water at 25 °C, K_a is the ionization constant of the corresponding substituted benzoic acid, ρ is a constant for the specific reaction and equal to 1 for the ionization of benzoic acids, and σ is the substituent constant, dependent on the substituent. The equation can be rewritten to solve for the σ-constant of the substituents on the benzene ring as

$$\Sigma\,\sigma = (pK_a - pK_a)/\rho \quad (3)$$

This form of the equation allows pK_a values to be used to calculate σ-constants for substituents that have not previously been determined such as pentafluorobenzene (peptide **8**) and the *ortho*-substituted benzene rings in peptides **15** and **16**. The σ-constant is written as a sum to represent multiple substituents on the same benzene ring as in peptide **8**.

Calculation of log *P* Values. To measure the hydrophobicity of the substituents at position 350, the log *P* or octanol/water partition coefficient was calculated using ACD/PhysChem Batch (version 8.14, Advanced Chemistry Development, Inc. (ACD/Labs), Toronto, ON, Canada, www.acdlabs.com, 2004) software. The corresponding substituted benzene molecule for each peptide analogue was used to calculate the log *P* values. The error for the calculated values is ±0.20.

NMR Sample Preparation. Rhodopsin was obtained from bovine retinae as reported previously.[32] The NMR samples contained peptide (5 mg/mL), R at 2 mg/mL, Buffer K (20 mM sodium phosphate (pH 7.5), 100 mM KCl, 0.1 mM EDTA, 1 mM DTT), and 10% D_2O. Control samples without R contained just peptide and buffer. The total volume in the NMR sample tube was 500 μL. R was photoactivated by 490-nm light produced by a 150-W Fiber Lite for 30 s.

NMR Spectroscopy. One- and two-dimensional proton spectra were collected at 4.0 °C using a Varian Unity INOVA-700 MHz NMR spectrometer, 7400-Hz spectral width. Phase-sensitive two-dimensional spectra were obtained with the hypercomplex method. The sequence-specific backbone and side chain proton resonance assignments were performed using a combination of 2D 1H-TOCSY[50] and 2D 1H-NOESY[51] NMR experiments that implement a WATERGATE sequence for solvent water suppression. The TOCSY experiment implemented a DIPSI spin lock for polarization transfer and utilized mixing times up to 100 ms. The NOESY spectra used a 2 × 280 × 1248 data matrix with 16 transients. The final data matrix size after zero filling was 1024 × 2,048 complex points. Spectra with mixing times of 100, 200, and 350 ms were collected with a 3 s postacquisition delay to assess NOE buildup and spin diffusion. For structure calculations, the 200 ms spectra were used. Data processing and analysis of all the NMR spectra were performed using the VNMR [version 6.1 (Varian Associates)] and Felix 2001 (Accelrys, Inc) software packages on Silicon Graphics Indy/R5000 and Sun workstations.

Structure Determination. Sequence-specific and stereospecific ^{1}H assignments were established in a computer-assisted manner by analyzing appropriate regions of the TOCSY and NOESY spectra of free peptide and peptide in the presence of R (dark-adapted) by using standard procedures.[52] Interproton distance restraints were obtained from the NOESY spectra in a semiautomatic manner using the software ARIA (Ambiguous Restraints for Iterative Assignment, version 1.2).[53−55] This software protocol integrates automated NOE assignment processes with structure calculation. It assigns ambiguous NOEs during the structure calculation using a combination of unambiguous distance restraints and an iterative assignment strategy. Additionally, ARIA also mitigates the problem of underestimation of distance restraints that may result from longer mixing times by simulating spin-diffusion networks. The NOE intensities are calculated from a given structure using numerical integration of differential equations that govern the relaxation process. Selected structures of an iteration serve as a template to calculate the NOE intensities, and these calculated NOE intensities are used to calibrate the distance restraints for the subsequent iteration. This process diminishes the inaccuracies of the target distances incurred by spin diffusion. The computational algorithm employed torsion angle simulated annealing followed by torsion angle and then Cartesian molecular dynamics cooling stages. Structural refinement was completed in a water shell.

The semiautomatic assignment of the distance restraints was performed using the assignment possibility output of the first iteration of the structure calculation. The chemical shift tolerances were set to 0.025 ppm for the proton dimensions. With each iteration, the 10 lowest energy structures were used as templates for the next iteration, and the seven best structures were used for restraint violation analysis. This process was repeated 3 times until no additional assignment was observed as the iterations progressed. The stereochemical quality and structural statistics of the final ensemble were determined using PROCHECK [56] and PROCHECK NMR.[57]

Statistical Analysis. Correlations between R*-binding affinity and peptide properties were determined using linear regression and correlation analysis in GraphPad Prism. *P* values were calculated, and a significance level of 0.05 (alpha value) was used.

Results and Discussion

Peptide Binding Studies. The binding of C-terminal G$_t$α peptides can be monitored by observing the increase in the amount of MII present after light activation in the presence of the peptide. This is calculated as the amount of "extra" MII. Light activation of rhodopsin creates an equilibrium between the MI and MII photointermediate states of the receptor. The MI intermediate dominates, but the presence of C-terminal G$_t$α peptides, or the entire G protein transducin itself, shifts the equilibrium so the MII intermediate dominates. This "extra" MII was measured as described in Materials and Methods, and

(49) Hammett, L. P. *J. Am. Chem. Soc.* **1937**, *59*, 96−103.
(50) Braunschweiler, L.; Ernst, R. R. *Journal of Magnetic Resonance (1969−1992)* **1983**, *53*, 521−528.
(51) Kumar, A.; Ernst, R. R.; Wuthrich, K. *Biochem. Biophys. Res. Commun.* **1980**, *95*, 1−6.
(52) Wüthrich, K. *NMR of proteins and nucleic acids*; Wiley: New York, 1986.
(53) Linge, J. P.; O'Donoghue, S. I.; Nilges, M. *Methods Enzymol.* **2001**, *339*, 71−90.
(54) Brunger, A. T. et al. *Acta Crystallogr., Sect. D* **1998**, *54 (Pt 5)*, 905−921.
(55) Nilges, M.; Macias, M. J.; O'Donoghue, S. I.; Oschkinat, H. *J. Mol. Biol.* **1997**, *269*, 408−422.
(56) Laskowski, R. A.; MacArthur, M. W.; Moss, D. S.; Thornton, J. M. *Journal of Applied Crystallography* **1993**, *26*, 283−291.
(57) Laskowski, R. A.; Rullmannn, J. A.; MacArthur, M. W.; Kaptein, R.; Thornton, J. M. *J. Biomol. NMR* **1996**, *8*, 477−486.

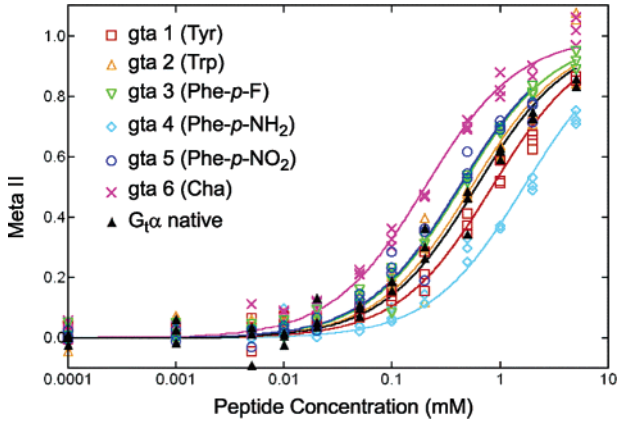

Figure 3. Dose responses of Meta II stabilization for the Series I peptides and $G_t\alpha(340-350)$ (Meta II is in arbitrary units). Measurements were fitted with the equation: Meta II = Baseline + Range × ([Peptide]/[Peptide] + EC_{50}) (Baseline = 0, Range = 1.0) to obtain EC_{50} values of the peptides.

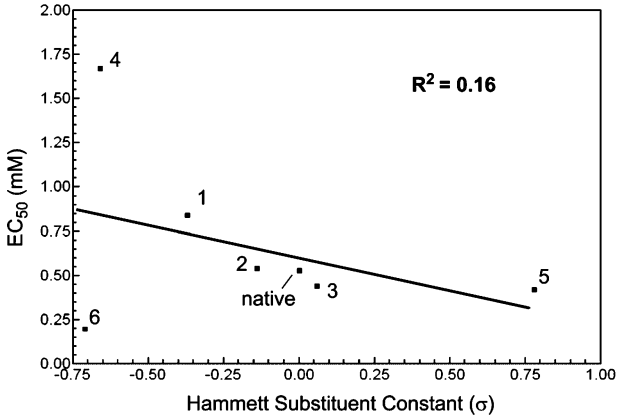

Figure 4. EC_{50} values of Series I peptides plotted as a function of the effective Hammett-substituent constant for the substituent on the aromatic ring at position 350. Best-fit line is calculated by linear regression (slope = −0.3780; intercept = 0.6067).

the apparent binding affinities expressed as EC_{50} values were calculated by fitting a dose−response curve of the Meta II values relative to peptide concentration with eq 1.

The fitted dose−response curves for Series I peptides are shown in Figure 3. Table 2 lists the calculated EC_{50} values for all peptides. Figure 4 is a plot of the EC_{50} values of native $G_t\alpha$-(340−350) and peptides **1**−**6** as a function of the effective Hammett substituent constant (σ) of the substituent on the aromatic ring at position 350. The electron density of the aromatic ring decreases as the Hammett substituent constant increases. The substituent constant for Cha (peptide **6**) was calculated by using the pK_a value of cyclohexanoic acid (4.91). Using eq 3 we get a σ-value of −0.71, indicating the relative electron density of the ring is higher than benzene (σ = 0.00). The substituent constant for Trp (peptide **2**) was calculated in a similar manner; the pK_a of 1*H*-indole-3-carboxylic acid is 4.06, giving a σ-value of −0.14.

Figure 5 shows the fitted dose−response curves for the peptides in Series II. The plot of EC_{50} values as a function of the Hammett-substituent constant for Series II peptides is shown in Figure 6; the Hammett constants for these peptides were calculated as described for Figure 4. Correlation plots of binding affinity versus hydrophobicity of the substituents at position 350 (expressed as log *P*) are shown in Figure 7.

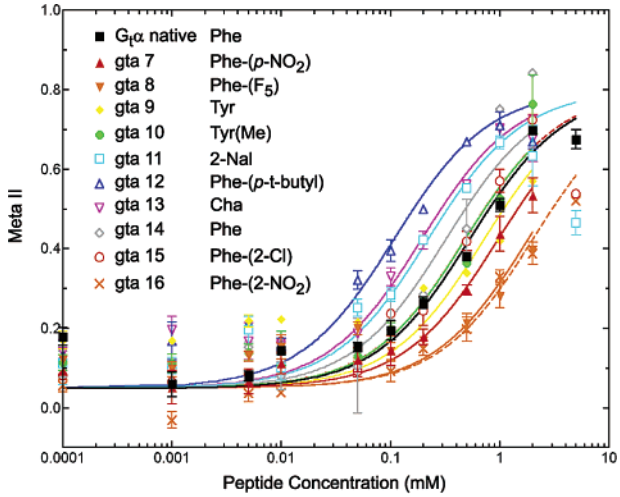

Figure 5. Dose responses of Meta II stabilization for the Series II peptides and $G_t\alpha(340-350)$ (Meta II in arbitrary units). Measurements were fitted as described in Figure 3 (Baseline = 0.05, Range = 0.75).

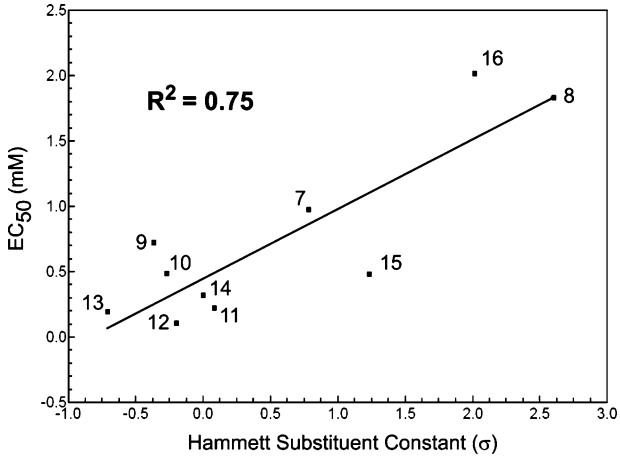

Figure 6. EC_{50} values of Series II peptides plotted as a function of the effective Hammett-substituent constant for the substituent on the aromatic ring at position 350. Best-fit line is calculated by linear regression (slope = 0.5298; intercept = 0.4652).

Carboxylate Peptides (Series I). Previous structure−activity studies using synthetic peptides and expression mutants[30,58] have shown that the carboxylate at the C-terminus of $G_t\alpha$ is important for maintaining binding affinity. As seen in the peptides of Series I, the electronic character (measured by Hammett-substituent constants, σ) of the side chain at position 350 has no correlation ($P > 0.05$) with the binding affinity of the α-peptide analogues (Figure 4, $R^2 = 0.16$); the EC_{50} values actually decrease as the electron density of the π-system decreases. If the cation−π interaction were helping to stabilize the receptor-bound conformation[46] of $G_t\alpha(340-350)$, one would expect to see the EC_{50} values increase as the electron density of the π-system decreases.

The peptides in Series I showed a good correlation ($P < 0.05$) between the hydrophobicity (calculated log *P* values) of the substituents and binding affinity of the peptides ($R^2 = 0.74$, Figure 7A). If peptide **5** is left out of the linear regression analysis, the correlation improves slightly ($R^2 = 0.80$, $P < 0.05$) (Figure 7A). The nitro substituent on this peptide appears to be involved in some unknown interactions that cannot be com-

(58) Osawa, S.; Weiss, E. R. *J. Biol. Chem.* **1995**, *270*, 31052−31058.

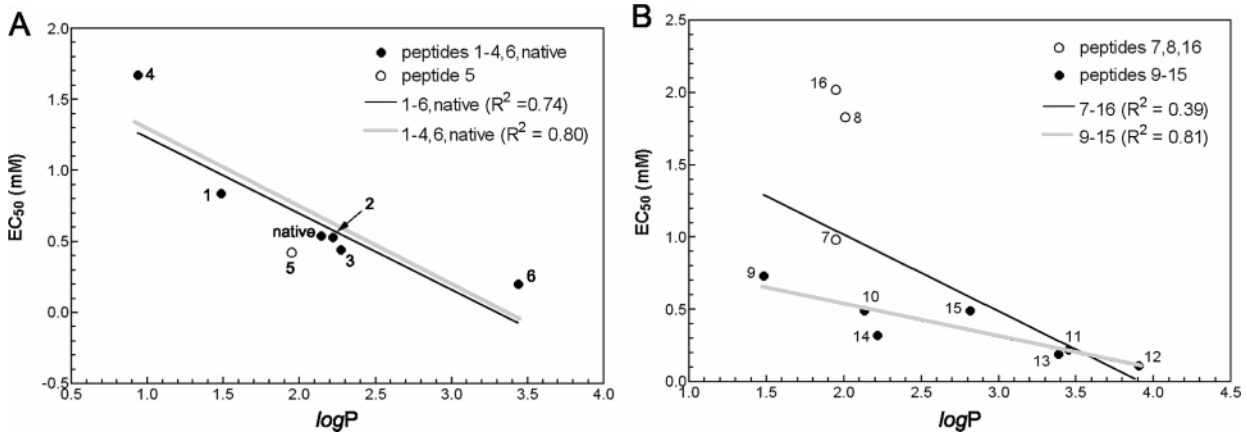

Figure 7. Correlation between binding affinity and log *P* for peptide analogues. EC_{50} values of Series I peptides plotted as a function of the log *P* of the side chain at position 350. Best-fit line is calculated by linear regression (GraphPad Prism). (A) Series I Peptides, black line (slope = −0.5359; intercept = 1.7680); gray line (slope = −0.5472; intercept = 1.842). (B) Series II Peptides, black line (slope = −0.5291; intercept = 2.0764); gray line (slope = −0.2255; intercept = 0.9890).

pletely described by the hydrophobic character of the substituent. As the log *P* increased, the binding affinity similarly increased suggesting, as does structure−activity data,[46] that increased hydrophobicity at the side chain of position 350 improves binding affinity. This is represented by peptide **6**, which contains the very hydrophobic Cha substituent and has the best EC_{50}, by a factor of 2, of any other peptide in the series.

Counterion Effect on Cation-π Interaction. In studies published after the binding affinities of the peptides of Series I were evaluated, Bartoli and Roelens[41] showed that the counteranion in a cation−π interaction has a dramatic effect on the estimated strength of the cation−π interaction. As conveyed in the Introduction, the study showed that anions with a diffuse charge (i.e., picrate) do not impact interaction strength as dramatically as anions with localized charge (i.e., acetate). In the G$_t$α peptide, the C-terminal carboxylate is the counteranion for the adjacent cation−π interaction between the ϵ-amine of Lys341 and the aromatic ring of Phe350. If the carboxylate of Phe350 reduced the energy contribution of the cation−π interaction to the level observed by Bartoli and Roelens[41] for the acetate anion (−0.6 kcal/mol in chloroform, and obviously less in a binding site with a larger effective dielectric), then it should be no surprise that a correlation was not observed between the experimental binding affinity and perturbations to the electronic density of the aromatic ring at position 350 in the Series I peptides. The salt-bridge formed between the Phe350 carboxylate and the ϵ-amine of Lys341 is a stronger interaction than the cation−π interaction in the native G$_t$α(340−350) peptide. This is essentially a restatement of simple Coulombic electrostatics; the energy of a salt-bridge (E_{sb}) is

$$E_{sb} = Q_{anion} \times Q_{cation} \quad (4)$$

where Q_{anion} is the charge of the anion and Q_{cation} is the charge of the cation (1 * 1 = 1), while the energy of a cation−π interaction ($E_{cation-\pi}$) is simply

$$E_{cation-\pi} = \partial Q_{\pi} \times Q_{cation} \quad (5)$$

where ∂Q_{π} is the partial charge of the aromatic ring. Therefore, $E_{cation-\pi}$ must be less than E_{sb} when scaled by the same environmental factors related to the effective dielectric constant and distances between the charges.

Carboxamide Peptides (Series II). Based on the study by Bartoli and Roelens,[41] we hypothesized that if the negative charge of the adjacent C-terminal carboxylate was eliminated, the cation−π interaction might be less shielded and more easily observed. To investigate this hypothesis, a series of peptides (Series II in Table 2) with the C-terminal carboxylate of Phe350 modified to a carboxamide were synthesized, thereby eliminating the localized charge of the carboxylate adjacent to the cation−π interaction, but obviously with another effective anion of undetermined type and location present experimentally.

The dose−response curves for this series of peptides (Figure 5) show the expected response to the change in electron density of the π-system of Phe350. Analogues with an electron-rich π-system (e.g., **11** and **12**) have lower EC_{50} values indicating tighter binding, and the analogues with electron-poor π-systems (e.g., **8** and **16**) have higher EC_{50} values indicating weaker binding to the receptor. Plotting the EC_{50} values as a function of the Hammett-substituent constants yields a very good linear correlation ($P < 0.05$) with $R^2 = 0.75$ (Figure 6). This positive correlation indicates that the cation−π interaction is observable by changes in the relative binding affinities and contributes to the stability of the R*-bound conformation of the peptides, but the absolute strength of its contribution remains undetermined. It is interesting to point out that peptide **14**, which only differs from the native peptide by the carboxamide at the C-terminus, binds and stabilizes MII better than the native peptide. This suggests that any loss of binding interaction by removal of the carboxylate's negative charge is balanced by restoration of the cation−π interaction.

NMR Studies and Structure of Peptide 14 Bound to R*. At first glance, one may question these conclusions, by asserting that the receptor-bound conformations of the peptides in Series I and II may differ. To address this issue, we determined a receptor-bound structure for peptide **14** (Series II) using TrNOE NMR experiments. First, we repeated the experiments with the native peptide (Series I) and R* in membranes and have confirmed the structure of Kisselev et al.[32] Then we used the same procedures to analyze peptide **14**. The sequential correlations between neighboring backbone amide and alpha protons used to help assign the peptide are illustrated in a NOESY walk in Figure 8A. The complete sequence-specific ^{1}H resonance assignments for peptide **14** are reported in Table 4. Note that

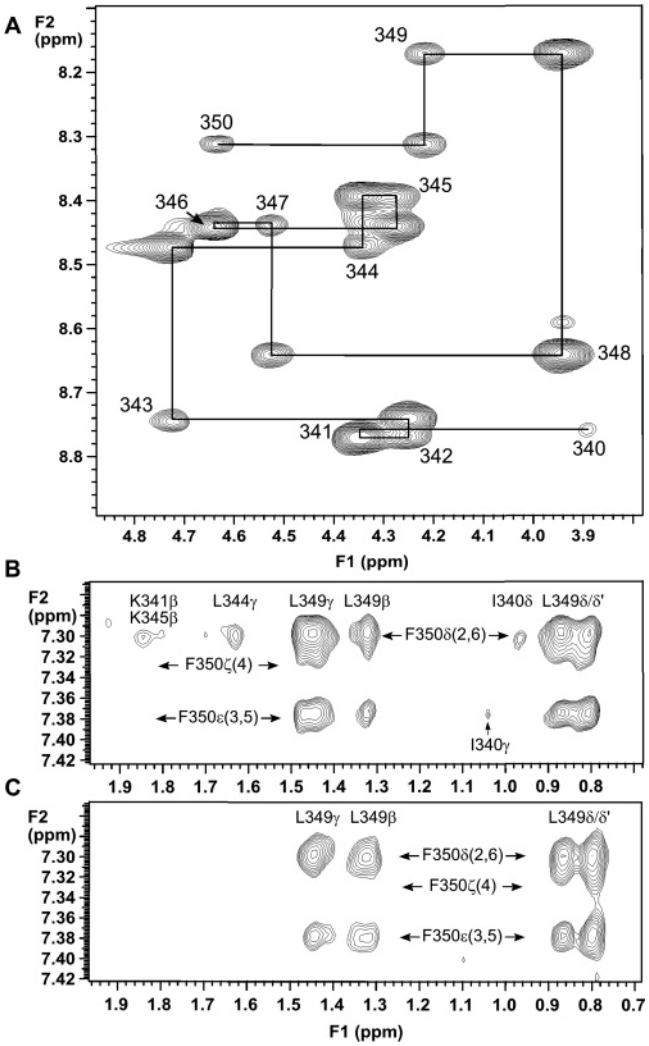

Figure 8. Selected regions from the 2D NOESY spectra of peptide **14** in the presence of rhodopsin. (A) The fingerprint region showing the intraresidue and sequential correlations used to help establish sequence-specific resonance assignments. The path over the sequential αH_i, NH_{i+1} connectivities is shown as a continuous black line. (B and C) A region showing aromatic (F2) − aliphatic (F1) NOE cross-peaks for the light-activated (panel B) and dark-adapted (panel C) states. Note the light-induced additional cross-peaks correlating the ring protons of Phe350 with those in residues at the other end of the peptide. These additional NOEs were not observed in the spectra of the dark-adapted samples, even at lower contour levels. A one letter code is used for amino acid annotations.

the C-terminal carboxamide modification gave rise to a new pair of correlated NH_2 resonances at 7.24 and 7.45 ppm. Also, the side-chain ammonium groups for Lys341/345 were visible in some spectra at 7.65 ppm, although these peaks were exchange broadened. Most importantly, the aromatic ring protons of Phe350 were completely resolved from all other proton resonances. This enabled the aromatic protons to serve as probes of local/global structure and to detect the presence of a cation$-\pi$ interaction.

Two-dimensional NOESY spectra for peptide **14** in the presence of rhodopsin are shown in Figure 8. A subset of the aromatic−aliphatic NOE correlations are illustrated for the light-activated (Figure 8B) and dark-adapted states (Figure 8C). Both spectra show strong NOEs resulting from the close proximity between the aromatic ring protons of Phe350 and the neighboring side chain protons of Leu349. However, only the light-activated state shows NOEs between Phe350 and residues at the other end of the peptide sequence: Ile340, Lys341/345, and Leu344. These weaker, long-range NOEs were reproducible and observed for two different sets of samples collected 4 months apart. For the dark-adapted state, there were no indications of any such long-range NOE cross-peaks. These NOEs indicate that the receptor-bound conformation of peptide **14** must adopt a structure that brings the N- and C-terminal residues into close proximity, similar to that of native peptide.

Table 4. Proton Resonance Assignments (ppm) for Peptide **14** at 4 °C and pH 7.5

residue	NH	αH	βH	γH	δH	others
Ile-340		3.90	2.00	1.51		γCH_2 1.24, γCH_3 1.03, δCH_2 0.95
Lys-341	8.76	4.36	1.86, 1.80	1.46	1.72	ϵNH_3 7.65, ϵCH_2 3.03
Glu-342	8.77	4.26	2.03, 1.95	2.29		
Asn-343	8.74	4.71	2.88, 2.77			γNH_2 7.75, 7.03
Leu-344	8.47	4.35	1.70	1.63		δCH_3 0.95, $\delta' CH_3$ 0.89
Lys-345	8.39	4.29	1.85, 1.81	1.46, 1.41	1.69	ϵNH_3 7.65, ϵCH_2 3.01
Asp-346	8.44	4.64	2.80, 2.70			
Cys-347	8.44	4.54	3.00			
Gly-348	8.64	3.95				
Leu-349	8.17	4.23	1.34	1.46		δCH_3 0.88, $\delta' CH_3$ 0.82
Phe-350	8.31	4.64	3.27, 3.02			δ(2,6)7.30, ϵ(3,5) 7.38, ζ(4) 7.33, C-terminal $CONH_2$ 7.24, 7.45

The R*-bound NMR structure of peptide **14** is shown in Figure 9. Independent calculations gave 20 structures with a high degree of convergence (Table 5 and Figures 9A, 10). The structure is almost identical to that of the native peptide as reproduced in the present study and originally observed by Kisselev et al.[32] It consists of a helical turn in the middle of the sequence spanning residues 3−7 followed by an open reverse turn (Figure 9). A representative structure of the ensemble was determined by calculating the mean coordinates in MOLMOL[59] and picking the structure from the ensemble that was closest to the mean coordinates of the ensemble. Superposition of the representative structure of peptide **14** to the representative structure of native $G_t\alpha(340-350)$ gives an RMSD of 1.4 Å for the backbone atoms, indicating an overall similarity (Figure 9C and D). The hydrophobic cluster of residues, Lys341, Leu344, Leu349, and Phe350, first observed in the native structure, is maintained in the structure of peptide **14**. One important difference between the structures of peptide **14** and native peptide is the rotation about the $C^{\alpha}-N$ bond of Phe350 that results in the carboxamide being oriented away from the peptide surface. This is most likely due to van der Waals violations that would occur if the carboxamide maintained the position and orientation observed in the native structure. Unlike the aromatic ring protons of Phe350, no long-range NOEs were observed between the carboxamide protons of Phe350 and protons more than three residues away in the peptide sequence, consistent with the carboxamide's orientation away from the surface of the structure.

Most importantly, the proximity of the ϵ-NH of Lys341 to the aromatic ring of Phe350 indicates the presence of a cation$-\pi$ interaction. The distance from the ϵ-amine nitrogen of Lys341 to the centroid of the aromatic ring of Phe350 is 3.07 ± 0.05

(59) Koradi, R.; Billeter, M.; Wuthrich, K. *J. Mol. Graph.* **1996**, *14*, 51−55, 29−32.

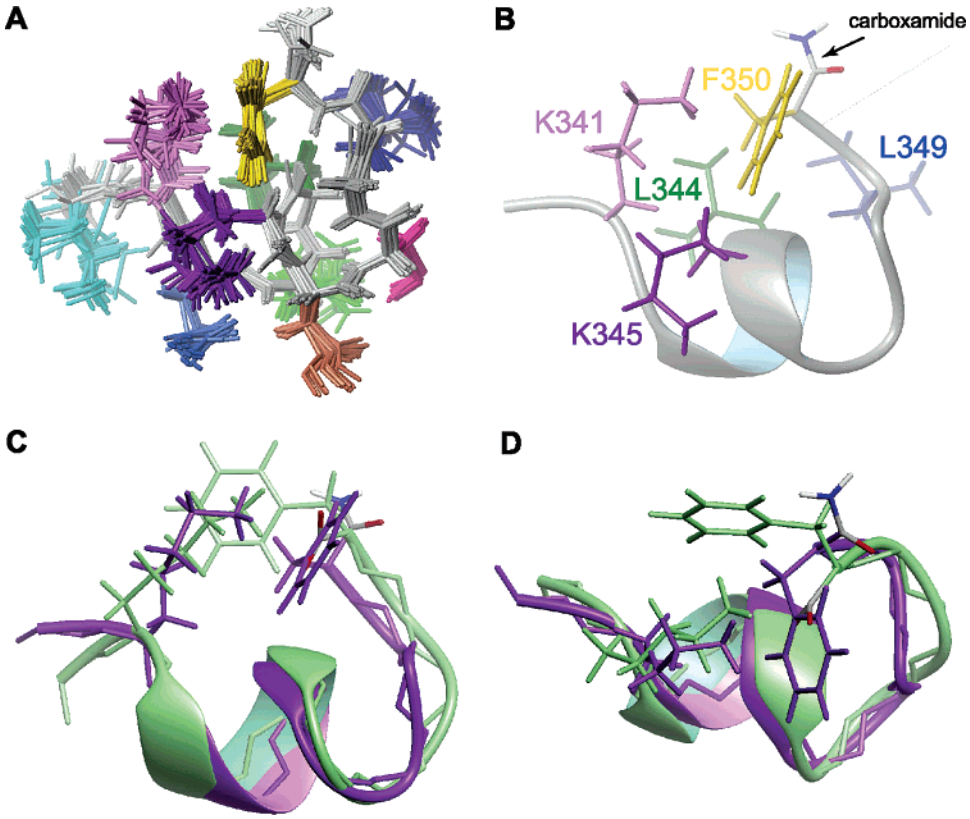

Figure 9. NMR structure of peptide **14** bound to R*. (A) Ensemble of 20 R*-bound structures computed independently. Backbone is in gray. Side chains are color-coded. (B) Ribbon diagram of R*-bound peptide **14** showing the hydrophobic cluster of residues and Lys345. Side-chain colors: Lys341, light purple; Leu344, green; K345, violet; Leu349, blue; Phe350, yellow. The carboxamide at the C-terminus is indicated, and the atoms are colored by atom type. Note that the proximity of the Lys341 amino group to the aromatic ring of Phe350 indicates the presence of a cation−π interaction. (C and D) Ribbon diagram of the representative structure of peptide **14** (purple) aligned with the representative structure of native $G_t\alpha(340-350)$ (green). Side view (C) and top view (D) of the molecules. (D) Note that the aromatic ring of Phe350 in peptide **14** occupies the same space as the carboxylate group of Phe350 in native peptide. The C-terminal groups of each peptide are colored by atom type. Structural images prepared with MOLMOL.[59]

Å. The NMR structure confirms the conclusion based on data from the MII stabilization assay showing the presence of a cation−π interaction in peptide **14**.

Hydrophobicity and Binding Affinity in Series II Peptides. It is necessary to address the binding affinity data for peptides **12** and **13** in the context of the other peptides. We know from the Series I peptides that the receptor favors peptides with hydrophobic residues at position 350. The *tert*-butyl group in peptide **12** is slightly electron donating and would be expected to improve binding if the cation−π interaction helps stabilize the bound conformation of the peptide. However, the degree to which we observe improved binding of peptide **12** cannot be simply explained by the electron-donating character of the substituent; it is more likely that the hydrophobic nature of the *tert*-butyl group is largely responsible for the dramatic increase in affinity observed. The same can be said for peptide **13** (3-fold increase in affinity) that contains Cha at position 350; the cyclohexyl group is more hydrophobic than the benzene ring of Phe (log *P* of 3.44 vs 2.13). The NMR studies of peptide **13** reveal a structure that is almost identical to that of peptide **14** and $G_t\alpha(340-350)$, except that the C-terminus does not fold back onto the helix. As might be expected, the inability to form a cation−π interaction leads to a more extended structure at the N- and C-termini. The ψ angle of Gly348 in **13** is rotated −81.7° from its position in **14**, the φ angle of Leu349 in **13** is rotated −117.7° from its position in **14**, and the ψ angle of Leu349 is rotated +168.4° from its position in **14**. This rotation results in the C-terminal two residues appearing rotated and flipped relative to peptide **14** following the helix-capping motif centered at Gly348 (Figure 11). The correlation between binding affinity and log *P* values of the substituents at position 350 for the Series II peptides was examined thoroughly. When data for all the peptides are used in the analysis, there is a marginal correlation ($R^2 = 0.39$, $P = 0.052$), but when the peptides with large electron-withdrawing substituents (peptides **7**, **8**, and **16**) are excluded, the correlation is very apparent ($R^2 = 0.81$, $P = 0.006$) (Figure 7B). These data lead us to speculate that the steric bulk of *these* peptides and/or the hydrogen bonding capability of the nitro groups of peptides **7** and **16** is influencing the R*-bound structure of the peptides. These unidentified interactions prevent the use of the hydrophobicity of the side chain of residue 350 as a simple predictor of R*-binding affinity for these three peptide analogues. However, one can conclude from the correlation for the other peptides in Series II that the hydrophobic nature of the residues influences binding affinity in addition to the "cation−π" and/or "salt-bridge" interactions.

Calculation of Cation−π Interaction Strength. Once a structure had been obtained of a peptide analogue, in which we had observed a cation−π interaction, we used the web-based version of the CaPTURE program [6] (http://capture.caltech.edu) to detect any cation−π interactions and determine their strength-(s). First, we ran the program on the original Kisselev et al.[32] TrNOE structure, and the program detected one energetically significant cation−π interaction between a Lys/Phe pair (Lys341-

Table 5. Statistics of the NMR Structure and Stereochemical Quality of Peptide **14**

ensemble RMSD values	all residues	reference value for X-ray structures (2.0 Å)
average pairwise C_α RMSD, Å	0.34 ± 0.16	N/A
average main-chain RMSD from mean coordinates, Å	0.60 ± 0.37	N/A

statistics	ensemble	reference value for X-ray structures (2.0 Å)
Ramachandran plot statistics		
residues in most favored regions [A,B,L], % (#)	62.5 (5)	75 ± 10
residues in additionally allowed regions [a,b,l,p], % (#)	37.5 (3)	
residues in generously allowed regions [~a,~b,~l,~p], % (#)	0.0 (0)	
residues in disallowed regions, % (#)	0.0 (0)	
main-chain statistics		
SD of ω angle, degrees	2.3	6.0 ± 3.0
bad contacts/100 residues	N/A	4.2 ± 10
Cα chirality, SD of ζ angle, degrees	1.2	3.1 ± 1.6
H-bond energy, kcal/mol	0.7	0.6 ± 0.2
side-chain statistics		
χ-1 gauche minus, degrees	17.8	18.1 ± 6.5
χ-1 trans, degrees	7.9	19.0 ± 5.3
χ-1 gauche plus, degrees	10.3	17.5 ± 4.9
χ-1 pooled, degrees	15.7	18.2 ± 4.8
χ-2 trans, degrees	29.5	20.4 ± 5.0

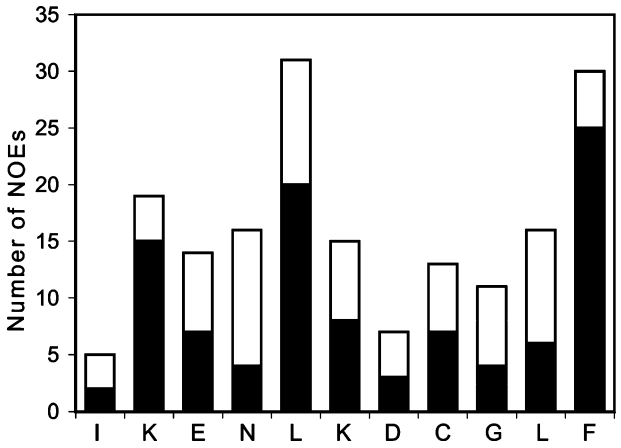

Figure 10. Distribution of distance restraints used for the calculation of the final ensemble of structures of R*-bound peptide **14**. Solid bars represent medium- and long-range interactions; open bars represent short-range NOEs.

Phe350), and the calculated interaction strength was −7.80 kcal/mol (E_{es}) (electrostatic energy component) and −0.85 kcal/mol (E_{vdw}) (van der Waals energy component). It was interesting to see that the interaction was so strong, yet unobservable by biological assay. Next, we ran the program on the structure of peptide **14**. The program again detected only one energetically significant interacting pair; a Lys/Phe pair (Lys2-Phe11, which corresponds to Lys341 and Phe350 in native peptide). The electrostatic energy component (E_{es}) was calculated as −7.95 kcal/mol, and the van der Waals energy component (E_{vdw}) was calculated as −0.36 kcal/mol. The calculated electrostatic energy difference between these two peptides is very small; this is curious considering the counterion in each system has to be different. Even if we say the counterion in peptide **14** is a simple

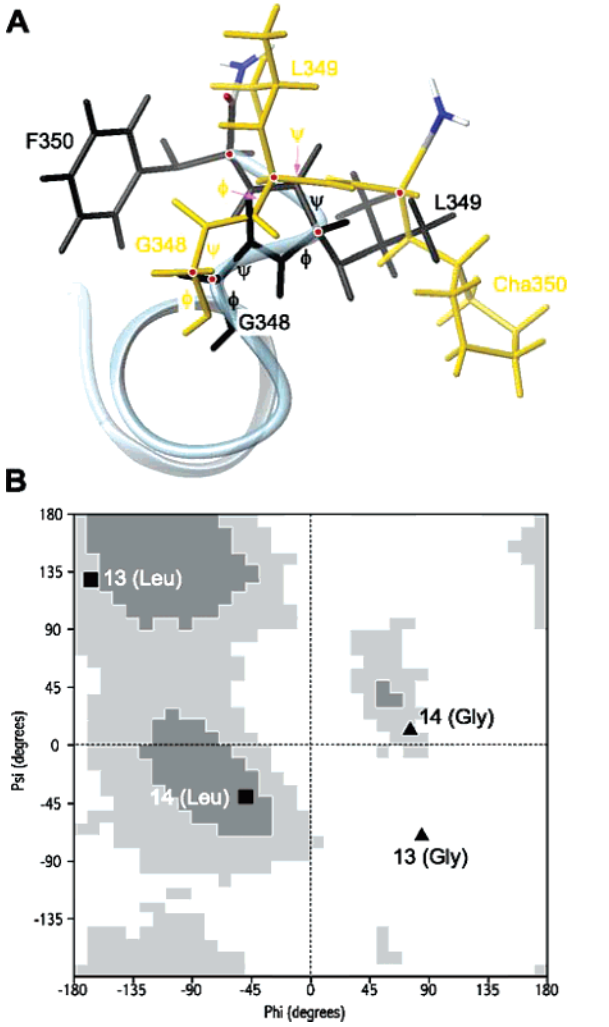

Figure 11. Comparison of NMR structures of peptides **14** and **13**. (A) Representative structure of peptide **13** (gold) superimposed on the structure of peptide **14** (black). Ribbon corresponds to structure of peptide **14**. Phi and Psi angles are indicated for the labeled residues. C^α carbons are indicated with red dots. Carboxamide groups are colored by atom type. (B) Ramachandran plot of Gly348 and Leu349 in peptides **13** and **14**. Shaded areas represent the various regions of torsional space: mostly favored (dark gray), additionally allowed (gray), generously allowed (light gray), disallowed (white). Plot generated with PROCHECK NMR.[57]

halogen ion, the ion with the strongest effect on cation−π interaction strength from the Bartoli and Roelens[41] studies had a measured interaction strength of −1.1 kcal/mol compared to −0.6 kcal/mol for the acetate ion. Assuming the correlation is accurate, the calculated interaction strength for the cation−π interaction in peptide **14** should be about −15 kcal/mol. Obviously, the CaPTURE program is not considering the influence of the adjacent counterion when calculating interaction energies. We acknowledge that the CaPTURE program is an effective tool for detecting cation−π interaction in peptides and proteins, but it does not calculate biologically relevant interaction energies, because there is always a counterion present in nature.

Relative Strengths of Cation−π Interactions versus Salt-Bridges. Decomposition of the impact of the salt-bridge on the cation−π interaction, versus other issues such as the desolvation of the ion pair in the salt-bridge, which probably accounts for the enhanced affinity of the carboxamide analogue **14** over native peptide, is not straightforward. The significant differences found in the literature on the relative strengths of cation−π vs

salt-bridge interactions are troublesome. In the native peptide and Series I peptides the salt-bridge is the dominating interaction. This trend was predicted by the studies of Gallivan and Dougherty,[37] but the interaction energies calculated for the cation−π (−6.2 kcal/mol) and salt-bridge (−19.7 kcal/mol) interactions in a proteinlike solvent environment were significantly higher than what has been observed experimentally. The consensus of numerous experiments in widely varying systems and solvents has been that a cation−π interaction only contributes −0.2 to −2.4 kcal/mol to substrate binding and/or peptide/protein stability.[3] One probable explanation for this discrepancy is the impact of the counteranion on the cation−π interaction suggested by Bartoli and Roelens[41] and by Hunter et al.[40] Omission of an explicit anion to counterbalance charge in the calculations of Minoux and Chipot,[60] Gallivan and Dougherty,[37] and Mo et al.[38] may well explain the much higher (approximately 3- to 10-fold depending on the anion) estimate on the interaction energy of cation−π interactions in their calculations regardless of the solvent environment.

Conclusions

In this study, we synthesized two series of peptides to explore the role of an observed cation−π interaction between the ϵ-amine of Lys341 and the aromatic ring of Phe350 in the C-terminal region of transducin's α-subunit. While there is geometrically a cation−π interaction in the native Gtα(340−350) peptide with an experimentally unobservable contribution to the stability of the receptor-bound conformation of the peptide, the adjacent salt-bridge between the Phe350 carboxylate and the ϵ-amine of Lys341 drastically minimizes any significant contribution of the cation−π interaction to binding affinity. Perturbation of the electron density of Phe350 was not detectable in the binding affinities of Series I peptide analogues in which the salt-bridge was present. As a result, the hydrophobic character of the side chain at position 350 played a dominant role in determining binding affinity. We have shown, however, that neutralization of the C-terminal carboxylate anion as the carboxamide in Series II peptide analogues revealed the cation−π interaction in binding-affinity measurements. Additionally, our NMR experiments have shown that peptide **14** adopts the same overall conformation upon binding R* as the Gtα(340−350) peptide and the cation−π interaction between Lys341 and Phe350 was preserved in the structure. Although we did not quantitate the absolute strength of the cation−π interaction, these studies provide experimental evidence that the relative strength of the cation−π interaction is sharply impacted by the adjacent counteranion. In addition, the salt-bridge dominates energetically over the cation−π interaction in the native peptide. Although this dominance has been predicted in the literature,[37] the interaction energies calculated in theoretical model systems lacking a counterion are inflated and not relevant to most experimental results. A probable explanation for the discrepancy between theoretical calculations and experimental determination of the strength of the cation−π interaction is, therefore, lack of explicit consideration of the anion associated with the cation.

Acknowledgment. Preliminary results on Series I analogues were presented at the 17th American Peptide Symposium.[61] This work was supported by grants from the NIH (EY12113, G.R.M.) and the Foundation for Research to Prevent Blindness and NIHRO163203 (O.G.K). R.A. was supported in part by the NIH training grant in Biophysics (GM008492). We also acknowledge the support of the Washington University Mass Spectrometry Resource Center partially supported by NIH (P41RR0954). This work was initiated during the thesis research of Dr. Rieko Arimoto and completed during the thesis research of Matt Anderson.

JA058513Z

(60) Minoux, H.; Chipot, C. *J. Am. Chem. Soc.* **1999**, *121*, 10366−10372.

(61) Sha, W.; Arimoto, R.; Marshall, G. R. In *2nd International/17th American Peptide Symposium*; Houghton, R. A., Lebl, M., Eds.; American Peptide Society: San Diego, CA, 2001.